Springer

Journal of Mechanical Science and Technology 23 (2009) 401~408

Journal of
Mechanical
Science and
Technology

www.springerlink.com/content/1738-494x
DOI 10.1007/s12206-008-1224-9

Effects of windowing filters in leak locating for buried water-filled cast iron pipes †

Young-Sup Lee*

Department of Multimedia Systems Engineering, University of Incheon, Incheon, 402-749, Korea

(Manuscript Received October 23, 2008; Revised December 19, 2008; Accepted December 30, 2008)

Abstract

Arrival time difference or time delay estimation is critically important for detection of leak location in buried water supply pipes. Because the exact leak locating depends upon the precision of the arrival time difference estimation between leak signals measured by sensors and the propagation speed of the leak-related elastic wave, the research on the estimation of time delay has been one of the key issues in leak locating. The arrival time difference was estimated with the peak time of cross correlation functions of the measured signals. In this study six different window functions, including the basic rectangular, Roth, Wiener, SCOT, PHAT and maximum likelihood windows were applied. Experimental results against an actual buried pipe made of cast iron showed that the introduction of the window functions improved the precision of time delay estimation. In this paper, a new statistical approach, that combines all results of each window function, is suggested for better leak locating. Apart from the experiment, an intensive theoretical analysis in terms of signal processing is described.

Keywords: Arrival time difference estimation; Buried water-filled pipe; Cross correlation function; Water leak location detection; Windowing filter

1. Introduction

Leak location detection of buried water pipes has mainly depended on the acoustical approach [1, 2]. This includes listening rods, hydrophones, ground microphones and correlators. Among these, the leak noise correlators are being used most widely, which are based on cross correlation functions of measured sensor signals since their suggestion in the 1970s [1-3].

It has been known that a leak signal propagates to both the longitudinal ends of a water-filled cast iron pipe from the leak location. The propagation of the leak signal is strongly coupled with elastic properties and dimensions of water, pipe structures and surrounding media such as soil and this leads to the leak signal possibly being dispersive, which represents the signal speed varying with frequency [3]. By the way, in a limited frequency range, the cross spectrum of the sensor signals is a linear phase with non-dispersive property. This indicates the leak signal speed can be constant over the limited frequency range. Hence the signal propagation speed against various pipes is usually provided with a table by leak correlator manufacturers, which was acquired by experiments [4].

In the determination of the time difference, the peak location of the cross correlation function calculated from the measured leak signals is crucial. However since the leak signal may be random and contaminated by noise, the peak location of the cross correlation function is not given easily in general [3]. Therefore, a number of the arrival time difference estimation methods have been studied by many researchers [5-10], and they have been used in many other applications such as a radar or sonar.

† This paper was recommended for publication in revised form by Associate Editor Eung-Soo Shin

* Corresponding author. Tel.: +82 32 770 8656, Fax.: +82 32 770 8760
E-mail address: ysl@incheon.ac.kr

Knapp and Carter suggested the generalized cross correlation (GCC) method to estimate the time delay between two signals [5]. Roth recommended a normalized cross spectrum [6], and Hero and Schwartz showed the so-called Wiener method for a better cross correlation function [7]. Also the smoothed coherence transform approach was studied by Carter et al to suppress unwanted tonal noise involved in measurement [8]. Brandstein and Silverman defined the phase transform to obtain a robust time delay estimation in reverberant signals [9], and suggested maximum likelihood filtering to enhance the time delay accuracy [10].

The purpose of the paper is to compare six different time delay estimation methods based on the cross correlation functions. The theoretical background is described in section 2, and the six different methods to estimate the arrival time difference are also compared. In section 3, experimental results and discussions are presented with actually measured data. Finally conclusions are written in section 4.

2. Theoretical background

2.1 Principle of leak location detection

As illustrated in Fig. 1, two sensors are installed with a certain distance D on a water-filled cast iron pipe with a leak point. The distances between the leak point to sensor 1 and sensor 2 are d_1 and d_2 respectively , and can be calculated by[1]

$$d_1 = (D - c \cdot \Delta t)/2$$
$$d_2 = (D + c \cdot \Delta t)/2 \quad (1)$$

where Δt is the leak signal arrival time difference between the two sensors and c is the leak signal propagation speed. It is usually difficult to identify the time difference just by comparing the measured two signal waveforms when the signals are deteriorated by various noises.

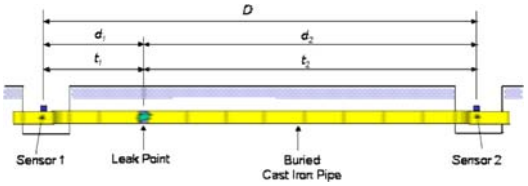

Fig. 1. Leak locating by the arrival time difference method with two sensors for a buried water-filled pipe.

2.2 Estimation of arrival time difference

The measured signals by sensor 1 and 2 are $x(t)$ and $y(t)$, respectively, as illustrated in Fig. 1 and can be expressed as,

$$x(t) = s(t) + n_x(t) \quad y(t) = \alpha s(t) + n_y(t) \quad (2)$$

where $s(t)$ is a pure leak signal. It is assumed that both signals $x(t)$ and $y(t)$ are stationary random white noise with zero-mean. The amplitude factor α depends on the distances from the leak location to sensors, and $n_x(t)$ and $n_y(t)$ are both noises measured by each sensor. One of the arrival time difference estimation methods is to use the cross correlation function $R_{xy}(\tau)$ which can be defined as

$$R_{xy}(\tau) = E[x(t)y(t+\tau)] = \alpha R_{xx}(\tau - \Delta t) + R_{n_x n_y}(\tau) \quad (3)$$

where $E[\ ]$ is an ensemble average of the product of the two signals $x(t)$ and $y(t+\tau)$. Thus if the two signals are correlated and $\Delta t = 0$ in Eq. (3), then the cross correlation function $R_{xy}(\tau)$ is symmetric with respect to $\tau = 0$. However, a time delay exists; the peak of the function will appear at a certain time delay $\tau = \Delta t$. If $n_x(t)$ and $n_y(t)$ are not correlated each other, then $R_{n_x n_y}(\tau) = 0$. However, the peak detection of the cross correlation function tends to be difficult in colored noise. Because the noise makes the term $R_{n_x n_y}(\tau) \neq 0$ in Eq. (3), the true peak location $\tau = \Delta t$ of the function is very difficult to deter

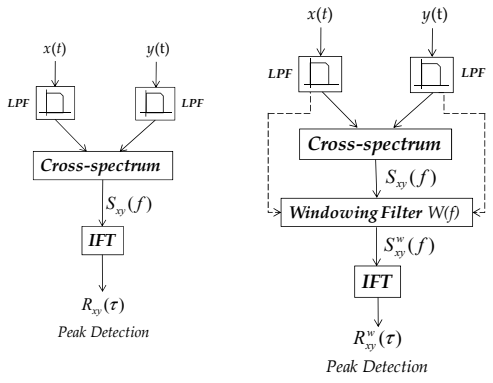

Fig. 2. Peak detection processes with the two measured signals. (a) Cross correlation function. (b) Application of windowing filter.

mine due to several other similar peaks around the true peak. In practice, thus, a low pass or band pass filter could be applied as shown in Fig. 2(a).

2.3 Generalized cross correlation function

Knapp and Carter introduced the generalized cross correlation (GCC) method to obtain a more organized framework for the estimation of the time difference [5]. The generalized cross correlation function with a weighting, $R_{xy}^{w}(\tau)$, can be defined as

$$R_{xy}^{w}(\tau) = w(\tau) * R_{xy}(\tau) \tag{4}$$

where $w(\tau)$ is a window function. Thus the windowed cross spectral density function, which is the Fourier transform of $R_{xy}^{w}(\tau)$, can be given as

$$S_{xy}^{w}(f) = \int_{-\infty}^{\infty} R_{xy}^{w}(\tau) e^{-j2\pi f\tau} d\tau = W(f) S_{xy}(f) \tag{5}$$

where $W(f)$ is the frequency domain version of $w(\tau)$ and $S_{xy}(f)$ is the cross spectral density function of the two measured signals of $x(t)$ and $y(t)$. Therefore, a number of researches have focused on investigating windowing filters after Knapp and Carter [6-10]. Since those windowing filters have been defined in the frequency domain, the GCC functions can be calculated by the inverse Fourier transform, as illustrated in Fig. 2(b), with

$$R_{xy}^{w}(\tau) = w(\tau) * R_{xy}(\tau) \tag{6}$$

Hence an improved peak location can be detected with the above GCC function.

2.4 Windowing filters

Six different GCC methods of improving the performance of a cross correlation are considered to prefilter the leak signals in the paper.

1) Basic rectangular window

The basic rectangular window method is the most fundamental way of calculating the cross correlation function between the two signals and can be useful to estimate the arrival time difference Δt. The window can be written as

$$W_B(f) = 1 \tag{7}$$

Thus, the windowed cross correlation function with the basic rectangular window can be given, from Eq. (5) and (6), by

$$R_{xy,B}^{w}(\tau) = \int_{-\infty}^{\infty} S_{xy}^{w}(f) e^{j2\pi f\tau} df = \int_{-\infty}^{\infty} S_{xy}(f) e^{j2\pi f\tau} df \tag{8}$$

2) Roth window

The Roth window method, which was proposed by Peter Roth [6], uses the inverse of the auto-spectrum of one measured signal from an accelerometer, for example $x(t)$, as can be defined by

$$W_R(f) = \frac{1}{S_{xx}(f)} \tag{9}$$

Thus, the windowed cross correlation function with the Roth window is the inverse Fourier transform of the normalized cross spectrum and can be obtained by

$$R_{xy,R}^{w}(\tau) = \int_{-\infty}^{\infty} S_{xy}^{w}(f) e^{j2\pi f\tau} df = \int_{-\infty}^{\infty} \left[\frac{S_{xy}(f)}{S_{xx}(f)} \right] e^{j2\pi f\tau} df \tag{10}$$

3) Wiener window

The Wiener window method, which is presented by Hero and Schwartz [7], estimates the cross correlation function by cross-correlating the least mean-square estimates of the signal component in each of the observed waveforms and is written by

$$W_W(f) = \gamma_{xy}^{2}(f) \tag{11}$$

where $\gamma_{xy}^{2}(f)$ is the coherence function. Thus the windowed cross correlation function with the Wiener window, $R_{xy,W}^{w}(\tau)$, can be given as

$$R_{xy,W}^{w}(\tau) = \int_{-\infty}^{\infty} S_{xy}^{w}(f) e^{j2\pi f\tau} df = \int_{-\infty}^{\infty} [\gamma_{xy}^{2}(f) S_{xy}(f)] e^{j2\pi f\tau} df \tag{12}$$

This approach can suppress the effect of the frequency range where the coherence is not good.

4) SCOT window

The SCOT (smoothed coherence transform) method, which is suggested by Carter et al [8] suppresses the unwanted consequences due to peaky tonal noises

in weak broadband signals such as leak noise. The window is defined as

$$W_S(f) = \frac{1}{\sqrt{S_{xx}(f)S_{yy}(f)}} \quad (13)$$

Thus the windowed cross correlation function in this method, $R^w_{xy,S}(\tau)$, is the inverse Fourier transform of the normalized cross spectrum divided by the SCOT window in Eq. (13) and can be given as

$$R^w_{xy,S}(\tau) = \int_{-\infty}^{\infty} S^w_{xy}(f) e^{j2\pi f\tau} df = \int_{-\infty}^{\infty} \left[\frac{S_{xy}(f)}{\sqrt{S_{xx}(f)S_{yy}(f)}} \right] e^{j2\pi f\tau} df \quad (14)$$

5) PHAT window

A frequency weighting function called PHAT window using the phase transform is defined by [9]

$$W_P(f) = \frac{1}{|S_{xy}(f)|} \quad (15)$$

Thus the windowed cross correlation function with the PHAT window, $R^w_{xy,P}(\tau)$, is expressed with

$$R^w_{xy,P}(\tau) = \int_{-\infty}^{\infty} S^w_{xy}(f) e^{j2\pi f\tau} df = \int_{-\infty}^{\infty} \left[\frac{S_{xy}(f)}{|S_{xy}(f)|} \right] e^{j2\pi f\tau} df \quad (16)$$

And it is known that it can remove the effects of the frequency characteristics of the physical system including sensors, leak sources and the leak propagation path.

6) Maximum likelihood (ML) window

The windowing filter in this ML window approach suggests enhancing the estimation accuracy of the time delay as suggested in Ref. [10] and is given as

$$W_{ML}(f) = \frac{\gamma^2_{xy}(f)}{[1-\gamma^2_{xy}(f)]|S_{xy}(f)|} \quad (17)$$

Thus the windowed cross correlation function with the ML window, $R^w_{xy,M}(\tau)$, is expressed with

$$R^w_{xy,M}(\tau) = \int_{-\infty}^{\infty} S^w_{xy}(f) e^{j2\pi f\tau} df = \int_{-\infty}^{\infty} \left[\frac{S_{xy}(f)\gamma^2_{xy}(f)}{[1-\gamma^2_{xy}(f)]|S_{xy}(f)|} \right] e^{j2\pi f\tau} df \quad (18)$$

This approach includes two pre-filtering operations and is usually applied when the measured signals are random Gaussian.

3. Experiment and results

3.1 Experimental set-up

A leak detection experiment for buried water-filled cast iron pipe (100A size) was carried out at a place in Daejeon, South Korea. The layout of the experiment site is illustrated in Fig. 3. It was an actual water supply pipe to the local area and buried about 1.5 m beneath the ground surface.

The distances between the two sensors for the three tests of the cast iron pipe were D = 174.1 m (d_1 = 110.6 m, d_2 = 63.5 m), 253.9 m (d_1 = 159.3 m, d_2 = 94.6 m) and 315.6 m (d_1 = 221.0 m, d_2 = 94.6 m) respectively. Two B&K 8313C accelerometers as leak signal detection sensors and a ball valve with 25 mm diameter controlling the water leak were installed on the pipe. The measured signals from the accelerometers were transferred to a B&K PULSE signal analyzer and B&K Nexus signal conditioners. Sampling frequency was 2048 Hz. Then the measured signals were recorded in the PULSE system. In the discussion, the case with the distance D = 174.1 m will primarily be described.

3.2 Measured leak signals and propagation speed

Fig. 4 shows the measured results of the leak test when D = 174.1 m. Fig. 4(a) presents the phase response of the two sensor signals, and the coherence function of $\gamma^2_{xy}(f)$ plotted in Fig. 4(b) reveals that the two measured signals are highly correlated in the frequency range of about 450 - 1000 Hz.

The relationship between the magnitude of the cross spectral density function $|S_{xy}(f)|$ and the phase $\phi_{xy}(f)$ in Fig. 4(a) can be given by [11]

$$S_{xy}(f) = |S_{xy}(f)| e^{j\phi_{xy}(f)} \quad (19)$$

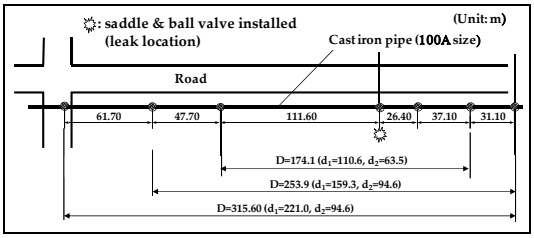

Fig. 3. Set-up for leak locating tests of the cast-iron pipe with the layout of the experiment site.

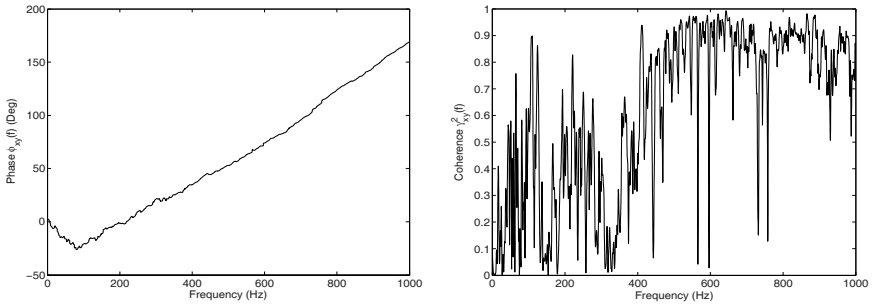

(a) (b)

Fig. 4. Measured signals properties. (a) Phase $\phi_{xy}(f)$. (b) Coherence $\gamma^2_{xy}(f)$.

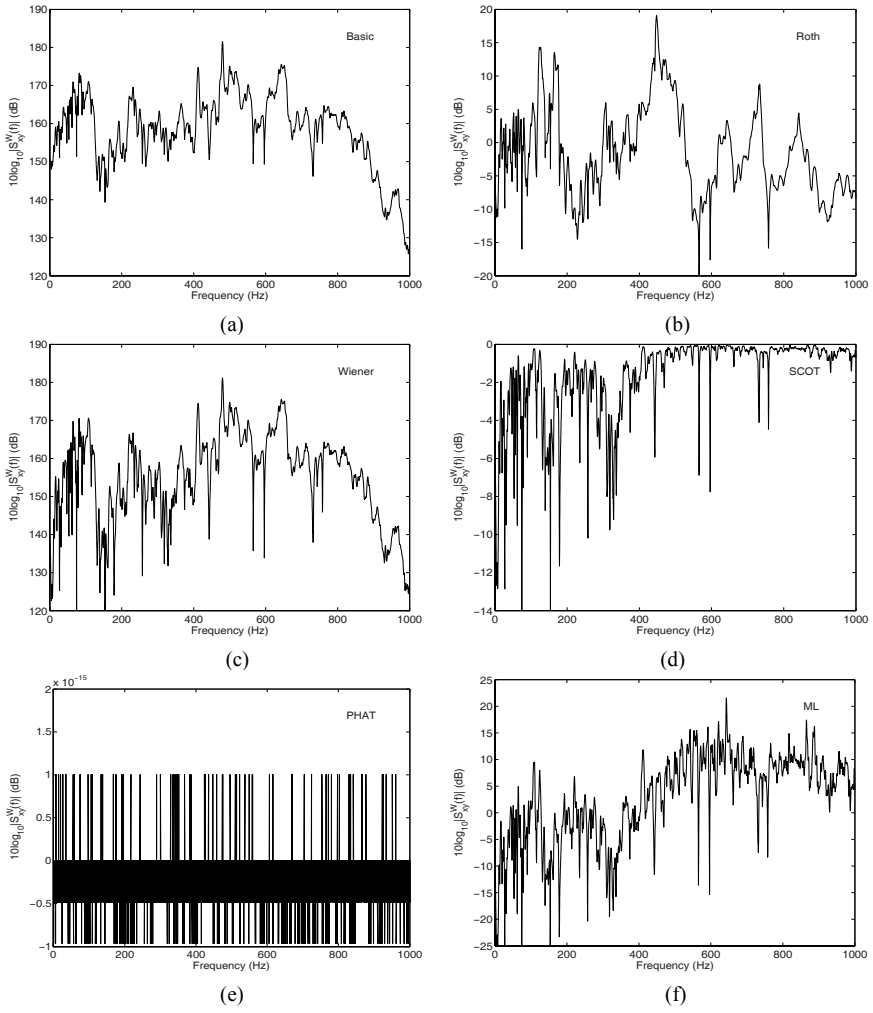

(a) (b) (c) (d) (e) (f)

Fig. 5. Windowed cross powerspectra $S^w_{xy}(f)$. (a) Basic rectangular window. (b) Roth. (c) Wiener. (d) SCOT. (e) PHAT. (f) ML.

Especially, the phase plot implies the response is a *linear phase* between 100 - 1000 Hz and can be expressed as

$$\phi_{xy}(f) = -\beta 2\pi f \tag{20}$$

where β is a constant. In a perfect linear phase system,

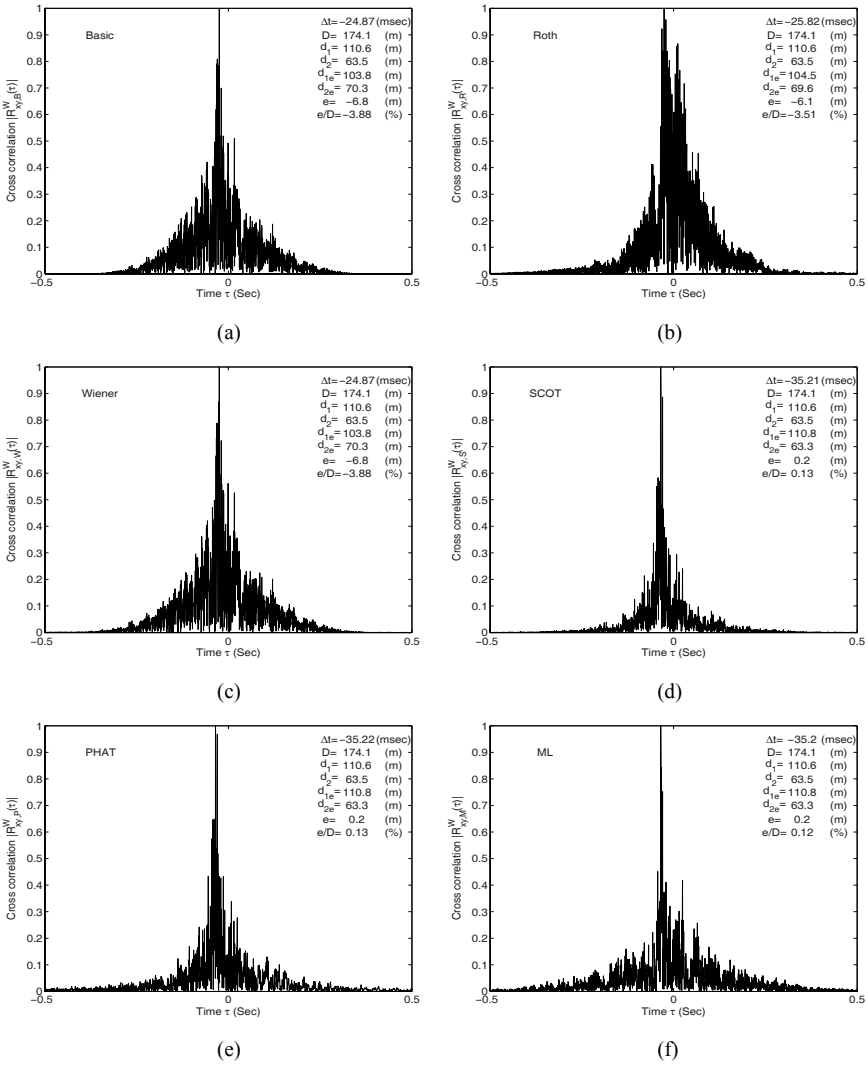

Fig. 6. Normalized absolute cross correlation function $|R_{xy}^{w}(\tau)|$ for the cast iron pipe. (a) Basic window. (b) Roth. (c) Wiener. (d) SCOT. (e) PHAT. (f) ML.

the phase delay between $x(t)$ and $y(t)$ is the same as the group delay, the relationships in the entire frequency range can be given as

$$\tau_g = -\frac{d\phi_{xy}(f)}{2\pi\, df} = \tau_p = -\frac{\phi_{xy}(f)}{2\pi\, f} \tag{21}$$

If the measured phase response in the limited frequency range of 100 - 1000 Hz is linear, the slope β in Eq. (20) is identical to the two delays in Eq. (21) and can be interpreted as time difference Δt between the two measured sensor signals. After some manipulation with the least square method, the slope of the phase as a straight line in the specific frequency range is obtained as β = - 0.0349 and $\beta = \tau_p = \tau_g$. From Fig. 4(c), the group delay $\tau_g = -\Delta\phi_{xy}(f)/2\pi\Delta f$ = - 200 (deg) / 2π * 900 (Hz) = - 34.9 (ms) is constant over the limited frequency range, so the group velocity and the phase velocity are identical and constant as well. The leak signal propagation speed can be obtained as $c = (d_2 - d_1)/\Delta t = (d_2 - d_1)/\tau_g$ = (63.5 - 110.6) / - 0.0349 ≈ 1350 (m/s) for the pipe.

3.3 Windowing filters and windowed cross spectra

Fig. 5 shows six different windowed cross spectral density functions $S_{xy}^{w}(f)$. In Fig. 5(a), $S_{xy}^{w}(f)$ with

the basic rectangular filter has resonances at around 100, 500 and 650 Hz. $S_{xy}^{w}(f)$ with Roth filter as shown in Fig. 5(b) has some more peaky resonances and anti-resonances. As can be seen from Fig. 5(c), $S_{xy}^{w}(f)$ with the Wiener filter is very similar to that with the basic filter especially at 450 - 1000 Hz. $S_{xy}^{w}(f)$ with the SCOT filter is plotted in Fig. 5(d), which looks like the coherence function in Fig. 4(b). $S_{xy}^{w}(f)$ with the PHAT filter in Fig. 5(e) looks quite different from the others because $10\log_{10}|S_{xy}^{w}(f)| \approx 10\log_{10}1 \approx 0$ and the variance in magnitude is very small. From Fig. 5(f), $S_{xy}^{w}(f)$ with the ML filter has relatively small variance in magnitude compared to the others except that with the PHAT filter and this may provide more weighting at higher frequency ranges.

3.4 Cross correlation functions & leak locations

The absolute and normalized windowed cross correlation function, $|R_{xy}^{w}(\tau)/\max[R_{xy}^{w}(\tau)]|$ as illustrated in Fig. 6 was used to estimate the peak of $R_{xy}^{w}(\tau)$. The arrival time differences were identified from Fig. 6 as Δt = -24.87, -25.82, -24.87, -35.31, -35.22 and -35.22 ms after applying the basic, Roth, Wiener, SCOT, PHAT and ML methods, respectively. The estimated d_1 is then calculated from Eq. (1), as d_{1e} = 103.8, 104.5, 103.8, 110.8, 110.8, and 110.8 m respectively as the true d_1 = 110.6 m. The ratios between the location error $e = |d_1 - d_{1e}|$ to D with the above six methods are e/D = 3.88, 3.51, 3.88, 0.13, 0.13 and 0.13 %, respectively. Hence, the SCOT, PHAT and ML methods showed the best performance with $e/D < 1$ %. By the way, the arrival time differences with the basic method and Wiener method are almost identical and this may be because $S_{xy}^{w}(f)$ in Fig. 5(a) and (c) are very similar as $|R_{xy}^{w}(\tau)/\max[R_{xy}^{w}(\tau)]|$ in Fig. 6 (a) and (c) are very similar. This indicates that, if noise can be ignored then $\gamma_{xy}^{2}(f) \approx 1$ from Eq. (11) and $W_W(f) \approx W_B(f)$; thus, the windowed cross correlation function becomes $R_{xy,W}(\tau) \approx R_{xy,B}(\tau)$.

Summarized test results are presented in terms of histograms in Fig. 7. Four measurements were carried out with each method. In Fig. 7(a), thus, 24 results to estimate leak location are plotted on a histogram when D = 174.1 m, and it is noted that 12 times of 24 results were observed at d_{1e} = 111 ± 1.0 m as the true d_1 = 110.6 m. In Fig. 7(b), the histograms of each individual method with four measurements are also plotted. The SCOT, PHAT and ML methods showed the exact leak location with 100 % hitting ratios, but the Roth method was the most inaccurate. By the way, the results with D = 253.9 m for leak locating were observed at d_{1e} = 159 ± 1.25 m and d_{1e} = 159 ± 2.5 m, respectively, as the true d_1 = 159.0 m. The results with D = 315.6 m were also observed at d_{1e} = 221 ± 1.5 m and d_{1e} = 221 ± 3.0 m, respectively, as the true d_1 = 221.0 m.

Therefore, it is concluded in the measurement against the cast iron pipe that the three better methods, say the SCOT, PHAT and ML methods, showed very stable accuracy of e/D < 1.0 % in leak locating whether the distance was less than 315.6 m. Also, the author suggests that a combined approach in terms of a histogram with all the three better windowing methods and multiple measurements could provide statistically more accurate and practical leak locating of buried water-filled pipes rather than choosing just one of the six methods.

As a discussion, it is critically important to know

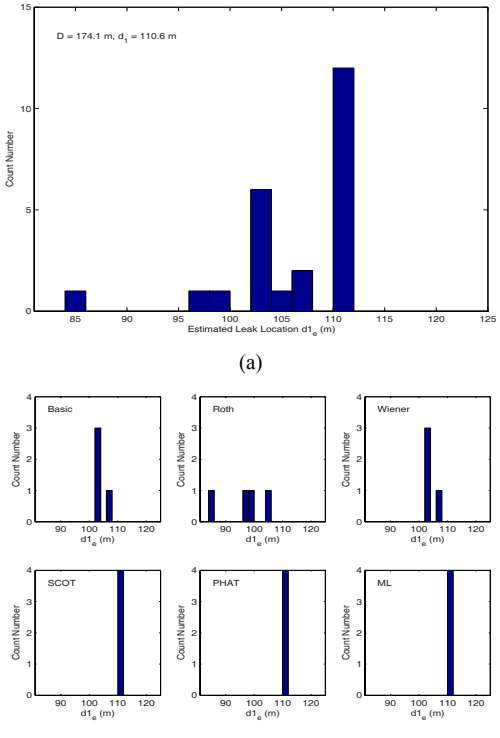

Fig. 7. Comparison of histograms of the leak location with the six different windowing filters. (a) Combined histogram. (b) Histograms of each method.

whether the measured noise signal is actual leak or not leak-related noise in a buried water-filled pipe. Basically, it is very difficult to detect leak locations by this approach if other excessive ambient noises with similar frequency property are involved. It is clear that this approach is available only when other ambient noises are removed or ignorable compared to leak noise level. In practice, noises such as a car passing, toilet flushing and construction noise are sometimes not continuous but temporal or intermittent. Leak signals, therefore, must be measured not once but several times with appropriate time intervals at the same pipeline. Then the possibility of wrong measurement especially due to temporal noises in leak detection could be much reduced. Also low pass or band pass filters are excellent for removing some ambient noises and finding leak locations.

4. Conclusions

Leak locating of buried pipe with the cross correlation function depends especially upon the accuracy of the arrival time difference between sensor signals. The arrival time difference estimation with the six different methods to detect the exact leak location of an actual buried water supply pipe made of cast iron is described theoretically and experimentally. Experimental results against an actual buried water supply pipe made of cast iron showed that the SCOT, PHAT and ML window methods gave outstanding leak locating capability as the errors were less than 1 % of the distance between the two sensors. Also a new statistical approach in terms of histograms with the combinations of all results is suggested for better practical leak locating.

References

[1] H. V. Fuchs and R. Riehle, Ten years of experience with leak detection by acoustic signal analysis, *Applied Acoustics*, 33 (1991) 1-19.

[2] E. Shaw Cole, Methods of leak detection: Overview, *Journal of American Water Works Association*, (1979) 73-75.

[3] Y.-S. Lee and D.-J. Yoon, Pinpointing of leakage location using pipe-fluid coupled vibration, *Journal of Korean Society for Noise and Vibration Engineering* (In Korean), 14(2) (2004) 95-104.

[4] Palmer Environmental, *MicroCorr*, Palmer Environmental Services.

[5] C. H. Knapp and G. C. Carter, The generalized correlation method for the estimation of time-delay, *IEEE Trans. Acoust., Speech, Signal Processing*, 24(4) (1976) 320-327.

[6] P. R. Roth, Effective measurements using digital signal analysis, *IEEE Spectrum*, 8 (1971) 62-72.

[7] A. O. Hero and S. C. Schwartz, A new generalized cross correlator, *IEEE Trans. Acoust., Speech, Signal Processing*, 33(1) (1985) 38-45.

[8] G. C. Carter, A. H. Nuttall and P. G. Cable, Proceedings of the IEEE, 61, 1497-1498, The smoothed coherence transform 61 (1973).

[9] M. S. Brandstein and H. F. Silverman, A robust method for speech signal time-delay estimation in reverberant rooms, *IEEE Conference ICASSP-97*, (1997) 1497-1498.

[10] E. J. Hannan and P. J. Thomson, Eliminating group delay, *Biometrika*, 60 (1973) 241-253.

[11] J. S. Bendat and A. G. Piersol, *Random Data*, John Wiley & Sons (1991).

Young-Sup Lee received his BS degree in Naval Architecture from Pusan National University, Korea, in 1987. He then received his MSc and PhD degrees from the University of Southampton, United Kingdom, in 1997 and 2000, respectively. Dr. Lee is currently an assistant professor at the Department of Multimedia Systems Engineering in the University of Incheon, Korea. His research interests include active control of sound and vibration, real-time signal processing, and smart sensors and actuators.